

# Multicomponent Synthetic Polymers with Viral-Mimetic Chemistry for Nucleic Acid Delivery

Mahmoud Soliman,<sup>†,‡</sup> Rujikan Nasanit,<sup>‡,§</sup> Samer R. Abulateefeh,<sup>†</sup> Stephanie Allen,<sup>†</sup> Martyn C. Davies,<sup>†</sup> Simon S. Briggs,<sup>§</sup> Leonard W. Seymour,<sup>§</sup> Jon A. Preece,<sup>‡</sup> Anna M. Grabowska,<sup>||</sup> Susan A. Watson,<sup>||</sup> and Cameron Alexander<sup>\*,†</sup>

<sup>†</sup>School of Pharmacy, University of Nottingham, Nottingham NG7 2RD, U.K.

<sup>‡</sup>School of Chemistry, University of Birmingham, Birmingham B15 2TT, U.K.

<sup>§</sup>Department of Clinical Pharmacology, University of Oxford, Oxford OX2 6HE, U.K.

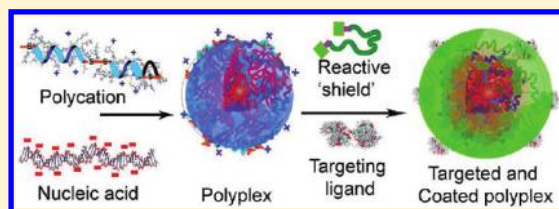
<sup>||</sup>Division of Pre-Clinical Oncology, University of Nottingham, Queens Medical Centre, Nottingham NG7 2UH, U.K.

<sup>‡</sup>Department of Pharmaceutics, Faculty of Pharmacy, Ain Shams University, Monazamet El Wehda El Afrikia St., El Abbassia, Cairo, Egypt

<sup>#</sup>Department of Biotechnology, Faculty of Engineering and Industrial Technology, Silpakorn University, Nakorn Pathom 73000, Thailand

## S Supporting Information

**ABSTRACT:** The ability to deliver genetic material for therapy remains an unsolved challenge in medicine. Natural gene carriers, such as viruses, have evolved sophisticated mechanisms and modular biopolymer architectures to overcome these hurdles. Here we describe synthetic multicomponent materials for gene delivery, designed with features that mimic virus modular components and which transfect specific cell lines with high efficacy. The hierarchical nature of the synthetic carriers allows the incorporation of membrane-disrupting peptides, nucleic acid binding components, a protective coat layer, and an outer targeting ligand all in a single nanoparticle, but with functionality such that each is utilized in a specific sequence during the gene delivery process. The experimentally facile assembly suggests these materials could form a generic class of carrier systems that could be customized for many different therapeutic settings.



**KEYWORDS:** multicomponent synthetic viral mimetics particles, DNA delivery, cross-linking polymers, acid cleavable spacers,  $pK_a$ -modulated polypeptides, RPCs

## 1. INTRODUCTION

Viruses are the most powerful current vectors for gene delivery, with an efficacy that still surpasses those of nonviral vectors.<sup>1–4</sup> They have functionality to enter specific cells, to escape endolysosomal compartments,<sup>5</sup> and to utilize cellular organelles and machinery to transport their nucleic acid cargoes where needed.<sup>6</sup> Many viruses have a highly organized core–shell structure, containing an outer coat to protect DNA or RNA in transit, and fusogenic peptides within their capsids to disrupt intracellular membranes. Viral vectors would be ideal for gene therapies but for concerns that they may induce adverse immune responses,<sup>7</sup> regain their virulence, or even induce cancer.<sup>8</sup> Many groups have sought to avoid problems with viral vectors by preparing synthetic carriers,<sup>9,10</sup> with a particular emphasis on polycations that can compact nucleic acids to particles similar in size to viruses and which can easily associate with cellular membranes before being taken up by cells.<sup>11</sup> Unfortunately, nonviral vectors generally have lower cellular uptake compared to viral counterparts,<sup>5</sup> while some nondegradable synthetic vectors have been found to exhibit toxicity. This has been attributed to the inability of metabolic pathways to remove nondegradable polycations, especially when

they possess high molecular weights.<sup>12,13</sup> As a result, there remains a pressing need for efficient and safe synthetic gene carriers.<sup>14–18</sup>

We have been focusing efforts to develop polymeric biomaterials that are inspired by viral component architectures and functionalities but which can be assembled from readily accessible and biocompatible synthetic building blocks. We designed gene delivery vectors based on a viral-mimetic core–shell architecture, comprising:

- (i) A bioreducible synthetic polypeptide core, which is both cationic in order to condense polyanionic nucleic acids and capable of fusing with and/or disrupting intracellular compartments in a transient manner;
- (ii) A coating layer of hydrophilic polymer, attached to the polypeptide core following condensation with nucleic acids but which contains linkages designed to cleave in the acidic endosomal compartments of cells;

**Received:** March 5, 2011

**Revised:** November 4, 2011

**Accepted:** December 5, 2011

**Published:** December 5, 2011

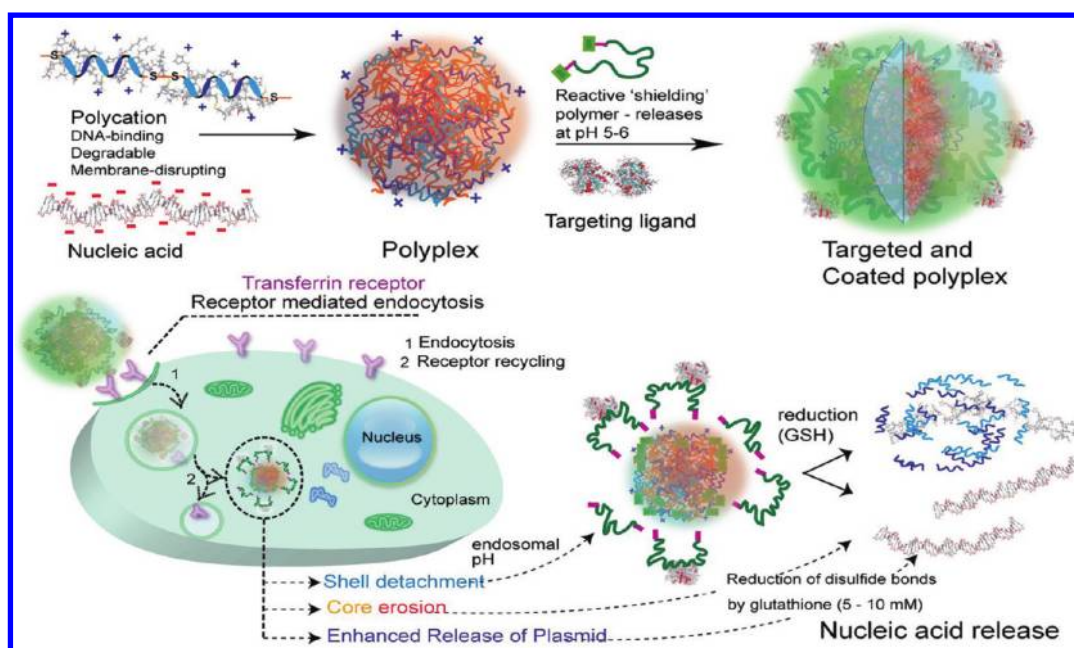


Figure 1. Schematic of modular synthetic gene delivery vectors.

- (iii) Cell targeting functionality cografted with the hydrophilic coating layer to direct the vector to an appropriate cell line.

The design concept is shown in Figure 1.

There have been a number of ingenious designs of gene delivery vectors that incorporate some of these individual components. Disulfide bonds and acid-labile groups, such as esters, phosphoesters, hydrazones, or acetals, have all been used to form reversible linkages in nucleic acid carriers that enable triggered release of drug cargoes from nonviral delivery vectors.<sup>19</sup> However, for condensing DNA efficiently into tightly compacted particles, excess polycations have generally been required in the carrier system, resulting in the formation of polycation–nucleic acid complexes (“polyplexes”) with high positive charge. The excess polycation has been shown to be responsible for the high *in vitro* transfection efficiency of some polyplexes,<sup>20</sup> but a covering of the positive charges on the resulting nanoparticle surfaces has been required before injecting the polyplexes into the systemic circulation. The reduction in overall positive charge of the polyplexes is needed to prevent interaction of the polycations with negatively charged plasma proteins, resulting in losses in bioavailability and gene carrying efficiency.<sup>21,22</sup> Furthermore, it has been suggested that injection of polycation/DNA systems that have not been additionally physically stabilized can cause swelling of the polyelectrolyte complexes and thus allow attack by serum nucleases during circulation in the bloodstream.<sup>23</sup> Controlled cross-linking of polyplex nanoparticles to provide physical stability and decrease overall surface charge has been achieved using a variety of reagents<sup>23–25</sup> as well as by hydrophilic polymers, e.g. pHPMA.<sup>26</sup> These not only reduced undesired interactions with blood proteins but also avoided early elimination of polyplexes by the reticuloendothelial system.<sup>27</sup> An adverse consequence of reducing the total surface charges was a decreased interaction with negatively charged membranes on the intended target tissue, preventing polyplexes from transfecting cells efficiently.<sup>25,28</sup> It should also be noted that

polyplexes coated with hydrophilic polymers have been shown to possess a lower ability to escape endosomal barriers, again resulting in a lower transfection efficiency.<sup>29</sup> As a consequence, enzyme-cleavable polyplex coating polymers,<sup>26</sup> or acid-cleavable PEG shields<sup>6</sup> linked to the polyplexes by hydrazones,<sup>30,31</sup> vinyl ethers,<sup>32</sup> orthoesters,<sup>33,34</sup> and acetals,<sup>29,35–38</sup> have all been considered as means to stabilize polyplexes without compromising their ability to interact with membranes and escape endosomal barriers.<sup>39</sup> In addition, some restoration of transfection efficacy has been achieved by tagging the hydrophilic cross-linking polymers covering the polyplexes with specific cell-surface receptor ligands.<sup>26,40</sup>

However, to date, there have not been reports where all the elements described above, i.e., bioreducible endosomolytic polypeptide cores, acid-cleavable coating polymers, and cell-specific surface-displayed retargeting ligands, have together been combined using biocompatible materials and chemistries amenable to fully aqueous syntheses. The materials we used to achieve this, based on reducible polycations (RPCs) and novel oxirane-terminated acetal-poly(ethyleneglycol) (PEG), are shown in Figure 2 together with atomic force microscopy (AFM) images of the noncoated and representative coated polyplexes. The specific rationales for the choice of these materials were also based on the modulation of charge afforded by the combination of lysine and histidine residues in the RPC core and variations for the coating polymers in their molar mass, number of reactive oxirane groups at chain termini, and ability to cleave from the polycation core through acid-degradable functionality.

## 2. EXPERIMENTAL SECTION

**2.1. RPC Synthesis.** Polypeptides were prepared as described previously.<sup>41</sup> The reaction mixtures were performed at various concentrations of the peptides (18, 30, and 60 mM). Peptides were dissolved in PBS (75 mM, 0.5X PBS) and 30% DMSO (~70 fold molar excess in respect to thiol groups) to form 18, 30, and 60 mM of the peptide concentrations in

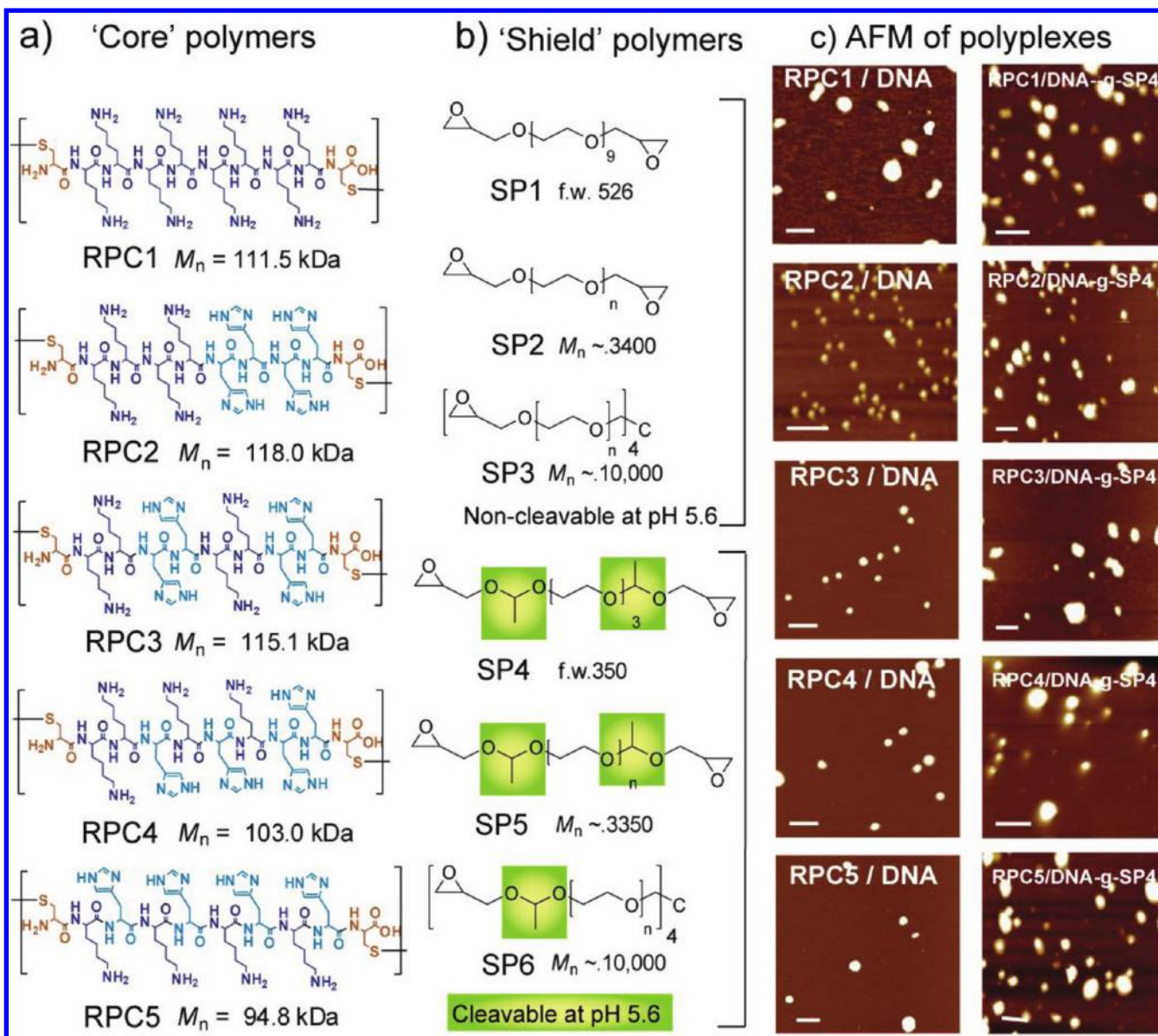


**Figure 2.** Chemical structures of core reducible polycation (RPC) polymers (a), coating or "shield" polymers (b) and AFM under aqueous conditions of noncoated and shield-polymer coated RPC/DNA complexes. The left-hand column of AFM images shows the complexes of RPCs with DNA alone, and the right-hand column shows the same complexes coated with shield-polymer SP4.

100  $\mu$ L total volumes. The reactions were incubated under ambient conditions. At varying time periods (0, 2, 4, 6, 8, 10, 12, 24, 30, 36, and 48 h), aliquots (5  $\mu$ L) were removed and the reaction quenched by adding 40  $\mu$ L of 17  $\mu$ M AET (2-aminoethanethiol). The progress of the polymerization was measured by monitoring the increase in molecular weight of the resulting polymer by gel permeation chromatography (GPC).

The quenched reactions were analyzed by size exclusion chromatography (SEC). The SEC analysis was performed using CATSEC-300 (250 mm  $\times$  4.5 mm ID) column eluted with 200 mM NaCl with 0.1% TFA. Ten  $\mu$ L of the samples were injected with 0.5 mL/min flow rate. Commercially available poly-L-lysine (PLL) (Sigma) samples (5–128 kDa) were used to estimate the molecular weight.

The reaction mixture was diluted in HEPES (15 mL, 15 mM, pH 7.4). The polymers were purified on centrifugal filter concentrators with molecular weight cutoff of 10000 (Centricon Plus 2, Amicon Bioseparation, Millipore, cellulose membrane,

UK). The mixture was centrifuged three times at 4000 rpm through the filters for this procedure. After the centrifugation steps, the molecular weights of the polymers, along with the removal of DMSO and other impurities, were verified by GPC.

**2.2. Synthesis of Coating Polymers SP4–6.** A set of polymers was designed and synthesized to check the effect of increasing polymer molecular weight (SP4 to SP6) and number of oxirane moieties per molecule (i.e., SP6) on polyplex cross-linking process.

**SP4.** Tri(ethylene glycol)divinyl ether (1.98 g, 9.79 mmol) was added to a magnetically stirred solution of glycidol (5 g, 48.96 mmol) in tetrahydrofuran (THF) (20 mL). The acid catalyst, pTsOH (95 mg, 0.5 mmol) was then added in three equal portions while the mixture was stirred in an ice-bath. The mixture was further stirred for 3 h at room temperature, and then saturated aqueous NaHCO<sub>3</sub> solution (8 mL) was added to quench the reaction. THF was evaporated under reduced pressure, and the remaining layer was extracted with 2  $\times$  10 mL

volumes of  $\text{CH}_2\text{Cl}_2$ . Organic extracts were dried over  $\text{Na}_2\text{SO}_4$  and the solvent evaporated under reduced pressure. This reaction yielded 1.5 g of impure product that was separated using column chromatography (using silica column pre-equilibrated and eluted by ethyl acetate:hexane 1:1 containing 2% (v/v) triethylamine). The oxirane-containing product separated as a pale-yellowish liquid, unoptimized yield after two chromatographic separations to obtain purified material was 0.1 g (5%).

**SP5 and SP6.** Glycidylvinyl ether (0.59 g, 5.9 mmol and 0.4 g, 4 mmol, respectively) solutions in THF (20 mL) were added to solutions of poly(ethylene glycol) or 4-arm PEG (0.34 g, 0.1 mmol and 0.3 g, 0.03 mmol, respectively) dissolved in THF (20 mL) with stirring, and then pTsOH (57.1 mg, 0.33 mmol and 114.2 mg, 0.66 mmol, respectively) were added in three equal portions while the mixture was stirred in an ice-bath. The mixtures were stirred for 3 h at room temperature before being quenched by adding saturated aqueous  $\text{NaHCO}_3$  solution (10 mL). THF was then evaporated under reduced pressure, and the remaining layer was extracted with  $2 \times 10$  mL volumes of  $\text{CH}_2\text{Cl}_2$ . Organic extract was dried over  $\text{Na}_2\text{SO}_4$ , and the products were purified by precipitation in diethylether ( $\text{Et}_2\text{O}$ ) and then vacuum-dried. The oxirane-containing product separated as a whitish powder; yields were 35 and 29%, respectively. The degrees of conversion of terminal hydroxyl groups of PEG to oxiraneacetal were calculated to be ~89.6 and 60%, respectively (calculated by  $^1\text{H}$  NMR).

SP1–3 as noncleavable analogues of SP4–6 were purchased from Sigma-Aldrich (SP1) and Creative PEG (SP2–3) and used as received.

### 2.3. Preparation and Characterization of Complexes.

pDNA was added to a microcentrifuge tube at a final concentration of 40  $\mu\text{g}/\text{mL}$  in HEPES buffer (500  $\mu\text{L}$ , 10 mM, pH 7.4). Calculated amounts of the RPCs, PLL, and PEI were prepared in 500  $\mu\text{L}$  of HEPES buffer and added to DNA to form polyplexes at the desired *N/P* ratios. We used *N/P* ratios of 5:1 for RPC/DNA and PLL/DNA complexes, as these were found to exhibit the best balance of transfection activity with cell viability across several cell lines in our prior studies.<sup>41</sup> For PEI/DNA complexes an *N/P* ratio of 10:1 was used based on previous reports of greater complex stability and transfection activity.<sup>42</sup> Solutions were mixed gently by pipetting them up and down several times and then allowed to equilibrate for at least 30–60 min at room temperature before being characterized or cross-linked. Freshly prepared solutions of cross-linking polymers SP1–6 in HEPES buffer (10 mM, pH 7.4) were then added to the polyplex solutions (in the range of 0.5–30 polymer oxirane groups to amine molar ratio), and cross-linking reactions were carried out at 30 °C for at least 2 h before termination by the addition of ethanolamine (to a final concentration 0.1% (v/v)).

For the preparation of Tf-targeted systems, freshly prepared solutions of SP5 (5.8 mg/mL) in HEPES buffer were added to the polyplex solution. Cross-linking reactions were carried out at 30 °C for 1 h, then Tf solutions were added at final concentrations of 2–200  $\mu\text{g}/\text{mL}$ , and the reaction was continued in an ice bath overnight before termination by the addition of ethanolamine. The polyplexes were separated from unbound polypeptide and unreacted cross-linking polymer by size exclusion chromatography using Sephacryl S-400 HR prepacked microspin columns (Pharmacia Biotech, Uppsala, Sweden) preconditioned with a single dose of 200  $\mu\text{g}$  of PLL in HEPES buffer to reduce nonspecific adsorption of polyplexes.

### 2.4. Transfection and Metabolic Activity Assays.

**SP1–6 Cross-Linked Polyplexes.** Prior to transfection, A549 and bEND.3 cells (ATCC, Rockville, MD, USA) were seeded in RPMI-1640 and DMEM, respectively, supplemented with 10% FCS in 12-well plates at a seeding density of  $7 \times 10^4$  cells/well and incubated at 37 °C and 5%  $\text{CO}_2$ . Twenty-four h after cell plating, noncross-linked and SP1–6 cross-linked polyplexes of RPCs1–5, PLL, and PEI with gWIZ-LUC (Aldevron, Fargo, USA) prepared in 1 mL of reduced serum medium (Opti-MEM I) were added so that the final pDNA concentration was 4  $\mu\text{g}/\text{mL}$  per well. Following incubation for 4 h, the transfection mixture was removed and cells were washed and covered with fully supplemented media (1 mL). Cells were then incubated for a further 48 h before quantifying the luciferase expression by using a luciferase detection kit (Promega, UK). Cellular protein contents were assayed by Bradford assay using bovine serum albumin (BSA) standards for comparison.

**Tf-Targeted Polyplexes.** HCT116 and HL-60 cells (ATCC, Rockville, MD, USA) were seeded in RPMI 1640 (10% FBS) and IMDM (20% FBS), respectively, at a cell density of  $10^5$  and  $5 \times 10^5$  cells per well, respectively, in 24-well plates. Prior to transfection, the media were removed and nontargeted and Tf-targeted polyplexes with gWIZ-LUC were added to cells (equivalent to 1  $\mu\text{g}$  DNA in 500  $\mu\text{L}$ ) in Opti-MEM I and incubated for 4 h at 37 °C and 5%  $\text{CO}_2$ . Then the transfection media were removed (centrifugation was needed for HL-60) and replaced with polyplex-free fully supplemented media. After 48 h, cells were harvested, lysed in passive lysis buffer (PLB, Promega), and luciferase activity was analyzed using the luciferase assay kit (Promega). Luminescence was recorded using a Fluostar Optima luminometer BMG (Labtech, Jencons-Pls).

**Metabolic Activity (MTS) Assay.** Cells were grown in fully supplemented RPMI-1640, DMEM, and IMDM as previously described in transfection experiments. Then  $10^4$  cells/well were seeded into a 96-well plate and incubated for 24 h. Cells were washed with PBS then noncross-linked, cross-linked, or Tf-targeted DNA polyplexes (gWIZ-LUC) formulated with different polycations were added to cells at a final DNA concentration of 500 ng per well in 50  $\mu\text{L}$  of Opti-MEM I. After 4 h, cells were washed with PBS, covered with 100  $\mu\text{L}$  of fully supplemented medium, and incubated for a further 72 h. The % cell viability was determined by adding 20  $\mu\text{L}$  of CellTiter 96 AQueous One Solution (Promega, UK) per well in 100  $\mu\text{L}$  of medium. Plates were incubated for further 4 h in humidified 5%  $\text{CO}_2$  at 37 °C after adding the reagent, then the absorbance at 490 nm was determined using a MRX Revelation microtiter platereader (Dynex Technologies, Chantilly, VA, USA).

**2.5. Instrumentation. Infrared Spectroscopy.** Infrared absorption spectra were obtained with a Nicolet spectrometer (Avatar 360 FT-IR spectrometer, Thermo Scientific, USA) under dry nitrogen at 25 °C, in transmittance mode at a resolution of 4  $\text{cm}^{-1}$ . Infrared analysis of acetal containing polymers (SP4–6) indicated characteristic peaks in the ranges of 2870–2886  $\text{cm}^{-1}$  (–alkyl C–H stretch), 1456–1467  $\text{cm}^{-1}$  (– $\text{CH}_2$ –,  $\text{CH}_3$ – bend), 1349–1359  $\text{cm}^{-1}$  (– $\text{CH}_3$  umbrella bend), 1280–1288  $\text{cm}^{-1}$  (–C–OH stretch), 1106–1112  $\text{cm}^{-1}$  (–C–O–C stretch) and 840–855  $\text{cm}^{-1}$  (–COCOC acetal–sym stretch). Small bands observed at 3467–3521  $\text{cm}^{-1}$  (weak O–H stretch), assigned to unreacted –OH groups (in SP5 and S6) or residual amount of water, which proved difficult to remove from these hygroscopic polymers.

**<sup>1</sup>H NMR Spectroscopy.** <sup>1</sup>H and <sup>13</sup>C NMR spectra were recorded on a Bruker 400 spectrometer at 399.8 MHz in CDCl<sub>3</sub> and D<sub>2</sub>O solutions. All chemical shifts are reported in ppm relative to TMS or DSS.

**Gel Permeation Chromatography.** Molar masses of SP4–6 were determined in chloroform using gel permeation chromatography. A single solution of each sample was prepared by adding polymer samples (3–5 mg) to 1 mL of chloroform with shaking to ensure complete dissolution of the sample. The solutions were then filtered (0.4 μm cutoff), and an aliquot (~500 μL) of each filtered solution transferred to glass sample vials. The vials were then placed in the instrument autosampler compartment and after an initial delay of 15 min to allow the samples to equilibrate to room temperature; injection of part of the contents of each vial (~100 μL) was carried out automatically. Molecular weights were calculated relative to PMMA or polystyrene calibrants. A Polymer Laboratories GPC 50 instrument equipped with PLgel guard plus 2× PL Mixed Gel-B column (30 cm × 10 μm) and a nominal flow rate of 1.0 mL/min was used at a temperature of 30 °C. The eluted polymer was detected with a differential refractometer. Data capture and subsequent data handling was carried out using instrument-associated Cirrus software.

The molecular weight and the polydispersity indices of the polymers 4–6 (summarized in Supporting Information Table S1) were determined by GPC (Supporting Information Figure S3). Determination of molar masses of polymers with reactive oxiraneacetal moieties was also verified by NMR in conjunction with the % conversion of polymer terminal groups to oxiraneacetals for the calculation of the amounts of the polymer to cross-link DNA polyplexes (i.e., oxirane equivalent weight).

**Atomic Force Microscopy.** Samples were prepared by adding 10 μL of noncross-linked and SP4–6 cross-linked RPC/DNA polyplexes (pEGFP-C1) to freshly cleaved muscovite mica. After 30 s, excess polyplex solutions were removed and then samples were washed twice with 200 μL of HEPES buffer (10 mM, pH 7.4). Samples were dried by exposing mica discs to dry filtered air for ~5 min before being imaged in air.

A Multimode AFM (Bruker Nano, Santa Barbara, CA), equipped with an E type scanner and NanoScope IIIa or V controller, was used throughout this study. The cantilevers used for imaging in air were silicon tapping probes (OMCL-AC160TS, Olympus) with a spring constant of 40–52 N/m operating at resonant frequencies of approximately 250–300 kHz. The tapping set points were adjusted to minimize probe–sample interactions. Topography images were plane-flattened and analyzed by using the computer software Nanoscope Software version 7.3 (Bruker Nano), or SPIP version 3.3.6 (Image Metrology A/S, Denmark).

**Fluorescence Microscopy.** Plasmid (gWIZ-LUC) was fluorescently labeled with the intercalating nucleic acid stain YOYO-1 by adding 1 μL of YOYO-1 (1 mM) to 200 μg of DNA (using a molar ratio of 1 dye molecule per 300 base pair). This was followed by agitating the complex for 1 h at room temperature and then labeled DNA was left in the dark for a further 2 h. Excitation and emission wavelengths for the dye are 491 and 509 nm, respectively. The labeled plasmid DNA was complexed as previously described.

For the fluorescence microscopy (FM) experiments, 12-well plates were seeded with  $1 \times 10^5$  HCT116 cells supplemented with RPMI-1640 containing 10% FBS. Cells were incubated at 37 °C and 5% CO<sub>2</sub> for 24 h. Then the medium was aspirated from the cells before washing cells with phosphate-buffered saline (PBS) and replaced with 1 mL of RPMI-1640 solution

containing polyplexes equivalent to 2 μg of gWIZ-LUC per well. SP5 cross-linked RPC2/gWIZ-LUC-YOYO-1 polyplexes and SP5 cross-linked RPC2/gWIZ LUC polyplexes targeted with Tf-FITC (amount equivalent to 2 μg of gWIZ-LUC) in 1 mL of RPMI-1640 were added on the top of HCT116 cells and incubated for 1, 4, 8, and 24 h. Cells were then washed twice with chilled PBS, fixed by adding 200 μL chilled freshly prepared paraformaldehyde (PFA, 1%(w/v)) after specified incubation times with polyplexes, and kept in a refrigerator prior to fluorescence microscopy investigation. For nuclei staining, 1 drop of DAPI standard stain solution was added to each well and the stain allowed to enter the cells over a period of 10 min. Cells were imaged using an inverted microscope (Leica DMIRB/E, Leica Microsystems, Germany), equipped with a fluorescence filters enabling DAPI, YOYO-1, and FITC imaging. Images were taken with a Leica DC200 camera and processed using the Leica DCviewer version 3.2.0.0 software. All microscopy gain and offset settings were maintained constant throughout the study.

**Dynamic Light Scattering.** Hydrodynamic radii of non-cross-linked, SP5 cross-linked, and Tf-conjugated RPCs and PLL/DNA polyplexes ( $N/P = 5$ ), and also PEI/DNA polyplexes ( $N/P = 10$ ), prepared using pEGFP-C1, were measured in HEPES (10 mM, pH 7.4) by recording scattered light at 90° to incident radiation in a Viscotek 802 dynamic light scattering (DLS) instrument equipped with a 50 mW internal laser operating at a wavelength of 830 nm. From standard auto correlation functions, measured diffusion coefficients were related to particles hydrodynamic radii via the Stokes–Einstein Equation. In addition, it was assumed that particles were spherical and noninteracting. Measurements quoted are the averages of triplicate samples measured as 10 replicates each. Radii quoted are averages for samples where >90% of the scattered light in terms of numbers of particles was from polyplexes within the size range quoted unless otherwise stated. To assess the kinetics of particle size growth of RPC/DNA polyplexes under reducing conditions, polyplexes equivalent to 10 μg of pDNA ( $N/P = 5$ ) were added to GSH (1 mL, 20 mM) in 10 mM HEPES buffer and the particle size was monitored over 4 h.

Cross-linking of RPC/DNA polyplexes produced only small changes in their particle sizes, and the SP5 cross-linked polyplexes maintained their particle sizes below 160 nm depending on the oxirane:amine (E:A) ratio (i.e., E:A < 15). However, the conjugation of Tf to SP5 cross-linked polyplexes was found to increase the particle size of cross-linked polyplexes (Supporting Information Figure S13), likely due to the conjugation of Tf to the polyplex surface during the cross-linking reaction resulting in particles with diameters in the range of 175–216 nm in diameter. The large increase in particle sizes of some Tf-targeted systems (e.g., RPC4 and PLL/DNA polyplexes), reaching a value of ~303 nm, may be attributed to the bridging and possible aggregation of polyplex particles, which are expected to be enhanced by the reaction of PEG oxirane terminals on the surface of different particles with amine groups of Tf.

**Zeta Potential Measurements.** Zeta potential ( $\zeta$ ) of noncross-linked, SP5 cross-linked and Tf-targeted RPCs and PLL/DNA polyplexes ( $N/P = 5$ ) and PEI/DNA polyplexes ( $N/P = 10$ ), prepared using ctDNA at concentration of 80 μg/mL, was measured using a Malvern Zetasizer 2000 equipped with a 10 mW He–Ne laser operating at a wavelength of 633 nm. Approximately 2 mL samples of freshly prepared polyplex solutions in PBS (10 mM, pH 7.4) were injected into

the instrument. Each sample was measured 5 times at room temperature to check for repeatability and  $\zeta$  potential (mV) was derived from the measured electrophoretic mobilities.

The tested polycation/DNA polyplexes were found to be positively charged with measured  $\zeta$  potential values ranging from +8.1 to +26.5 mV for RPC2 and PLL/DNA polyplexes, respectively (Supporting Information Figure S14). The conjugation of Tf to the surface of SP5 cross-linked RPC/DNA polyplexes caused a slight reduction in  $\zeta$  potential of tested polyplexes, as expected based on the net negative charge of transferrin at pH 7.4, reaching a minimum of +3.2 mV for Tf-targeted RPC3/DNA polyplexes; however, the differences between SP5 cross-linked polyplexes with and without conjugation to Tf were not statistically significant.

**Agarose Gel Electrophoresis.** Polycation/DNA polyplexes (gWIZ-LUC, 20  $\mu\text{g}/\text{mL}$ ,  $N/P = 5$ ) were prepared in HEPES buffer (10 mM, pH 7.4). Four  $\mu\text{L}$  loading dye (6X, Promega) was added to the samples (20  $\mu\text{L}$ ), and 5  $\mu\text{L}$  aliquots were loaded into agarose gel (1.0% (w/v) agarose in 0.5 X TBE buffer, stained with ethidium bromide 500 ng/mL). The gels were run at 110 V for 60 min in 0.5X TBE using an equal amount of gWIZ-LUC as a control loaded into gels along with polyplex samples. Gels were resolved on an electrophoresis cell (Fisher Scientific, UK), while an UV image station (Chemgenius, Syngene) was used to record and analyze gel images.

The stability of the noncross-linked polyplexes and polyplexes cross-linked with SP4 and 5 ( $N/P = 5$ , E:A ratio = 10) was studied initially using poly(aspartic acid) (PAA, DP = 105). The polyplex solutions were mixed with PAA (at concentrations equivalent to 5–80 times excess DNA), followed by overnight incubation at pH 7.4. Reversibility of cross-linking of polyplexes cross-linked with acid-cleavable SP4–6 was tested by acidifying cross-linked polyplexes to pH 5.6 with predetermined volumes of HCl (1M) measured using blank experiments. The acidified mixtures were mixed with PAA and incubated overnight (12 h) at ambient temperature before reneutralization with NaOH (1M) and loading into 1% (w/v) agarose gels. Gel experiments were run comparing dispersions of cross-linked polyplexes by the addition of predetermined amounts of PAA without and with acidification. Nontreated cross-linked polyplexes were used as negative controls, while cross-linked polyplexes, after overnight incubation (12 h) with PAA and 20 mM DTT at pH 5.6 for full polyplex dissociation before reneutralizing the mixtures, were also loaded into gels as positive controls.

**Hemocompatibility Assays.** Fresh blood from healthy human volunteers was collected in EDTA containing tubes, centrifuged at 4 °C for 3 min at 3000 rpm, and washed several times with phosphate buffered saline (PBS) at pH 7.4 until the supernatant was clear and colorless. Then 150  $\mu\text{L}$  of a 2.5% (v/v) suspension of the erythrocytes was mixed with 15  $\mu\text{L}$  of either the polycation (in the same final concentrations used to prepare polyplexes for transfection experiments i.e. 26.2–136.8  $\mu\text{g}/\text{mL}$ ) or the polyplex solutions, prepared in 5% (w/v) glucose/25 mM HEPES buffer in microcentrifuge tubes. After an incubation time of 60 min at 37 °C, the blood cells were removed by centrifugation, and the supernatant was transferred to 96-well plates.

The supernatant was then spectroscopically investigated at 570 nm with a MRX Revelation microtiter plate reader using 15  $\mu\text{L}$  of pure 5% glucose/HEPES buffer and 1% (w/v) Triton X-100 solution in water as negative and positive controls, respectively. Percentage hemolysis was calculated relative to

these controls according to the following equation.

$$\% \text{haemolysis} = 100 \times [(A_{\text{sample}} - A_{\text{blank}}) / (A_{\text{triton}} - A_{\text{blank}})]$$

**2.6. Statistical Analyses.** All of the data represent mean values  $\pm$  standard error of independent measurements. Statistical analysis was performed with a Student's *t* test and one-way ANOVA followed by the Tukey–Kramer post-test (GraphPad InStat software). Differences were considered as significant when  $P < 0.05$  (95% confidence level).

### 3. RESULTS

**3.1. Polypeptide Core Components and DNA Complexes.** Reducible polycations (RPCs 1–5, Figure 2) with histidine and lysine sequences linked via cysteine termini, prepared as previously reported,<sup>41</sup> were condensed with plasmid DNA encoding luciferase (gWIZ-LUC) under conditions ensuring a stoichiometric excess of amine groups. Dynamic light scattering (DLS), AFM, and  $\zeta$  potential measurements indicated that the resultant complexes were comparable in size, charge, and overall structure to those prepared in our previous studies.

**3.2. Shield Coating Polymers and Protection/Release of DNA.** Noncleavable bis- and tetra(oxirane)PEG shield polymers (SP1–3) and acid-labile bis- and tetra(oxirane)-acetal terminated PEGs (SP4–6), synthesized through modification of methods described by Fitton et al.,<sup>43</sup> were reacted with preformed RPC/DNA complexes under ambient conditions to generate the coated polyplexes. Gel retardation assays and AFM (Figure 3) confirmed that the cleavable shield polymers protected DNA in bound complexes, but released the nucleic acid under conditions of endosomal pH (5.6), while the core RPCs were able to liberate DNA under reducing conditions.

Further confirmation of the acid-cleavable behavior of the oxiraneacetal–PEG coating polymers, their ability to protect DNA in RPC complexes against stability challenges, and of the differences between coating of RPC/DNA complexes by SP1–3 (noncleavable) and SP4–6 (cleavable) were obtained by <sup>1</sup>H NMR, DLS, and  $\zeta$  potential analysis (Supporting Information).

**3.3. Transfection Assays: A549 and bEND.3 Cells.** RPCs 1–5 complexed with pDNA (gWIZ-LUC) were incubated with human lung carcinoma A549 and mouse brain endothelial bEND.3 cells either as native complexes or coated with noncleavable (SP1–3) or cleavable (SP4–6) polymers (Figure 4). We chose A549 epithelial cells as a representative of most types of common cancer and bEND.3 cells as an appropriate model for surfaces that are accessible following administration of polyplexes into the bloodstream. Transfection conditions ( $N/P$  ratios, cell seeding densities, incubation times) were adapted from our optimized prior protocols<sup>41</sup> to allow comparison of polymer-coated RPC complexes compared to RPC/DNA complexes across the range of lysine–histidine copolymer RPCs.

For A549 cells, the general trend across the sample set was that the highest transfection levels were obtained for the noncoated complexes and complexes coated with the acid-labile polymers SP4 and SP5, while reduced luciferase expression occurred for complexes coated with SP1–3 (noncleavable) polymers. Statistically significant ( $p < 0.05$ ) reductions in light production were observed for RPCs 1–5/DNA complexes when coated with noncleavable polymers SP1–3 compared to the native polymer/DNA complexes, with the exception only of

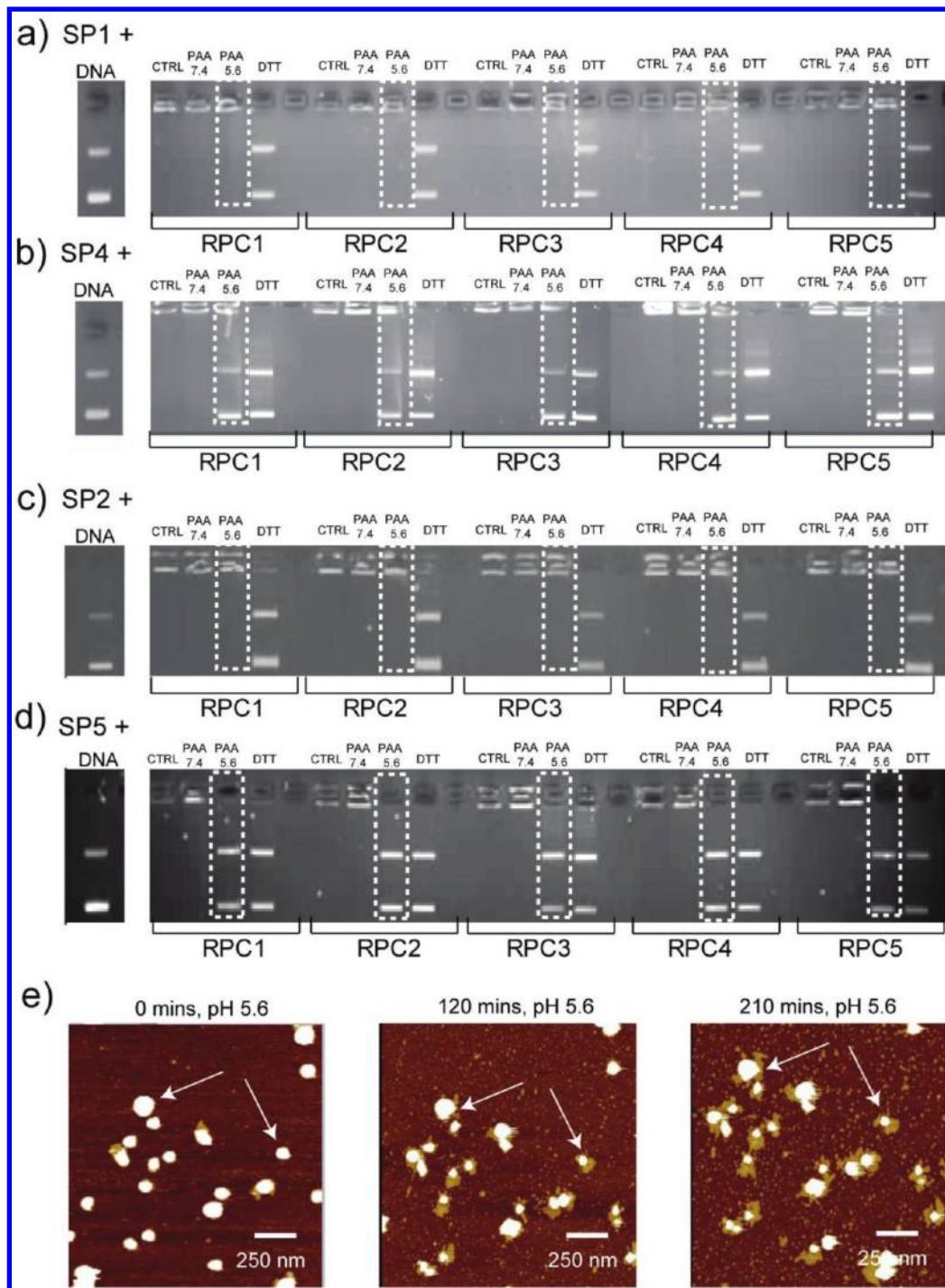


**Figure 3.** Gel retardation and AFM assays to show differences in stability of representative noncleavable (SP1, SP2) vs cleavable (SP4, SP5) coating polymers and unpackaging of DNA from RPCs. RPCs 1–5 coated with SP1 (a) and SP2 (c) retain DNA in their complexes under challenge by polyaspartic acid (PAA) at pH 7.4 and 5.6 (lanes 2 and 3 for each RPC) but release DNA on exposure to reducing agent dithiothreitol (DTT, lanes 4 for each RPC). (b,d) The same assays are carried out on RPCs 1–5 coated with acid-labile SP4 and SP5, where DNA release can be observed in lane 3 for each RPC, indicating loss of coating polymer and destabilization of the complex by competing PAA at pH 5.6 only. (e) The unpackaging under acidic conditions of DNA from RPC1 coated with SP5 is shown.

RPC3/DNA coated with SP2. Importantly, there were no significant differences in transgene expression for RPCs 1–5/DNA complexes when coated with acid-labile polymers SP4 and 5 compared to the native polyplexes. These differences were broadly as expected owing to the differences in lateral stabilization afforded by the cross-linking of the outer shell by the non acid-labile compared to the acid-labile bis(oxirane)PEG coating

polymers. However, it should be noted that there were a small number of individual variations to the trend, for example RPC3/DNA coated with SP4 was not as effective as the same polymer/DNA complex coated with SP5, and complexes coated with the degradable polymer SP6 were less effective transfection reagents than those with SP4 and SP5. We attribute the reduced transfection afforded by SP6 coated polymers to a greater

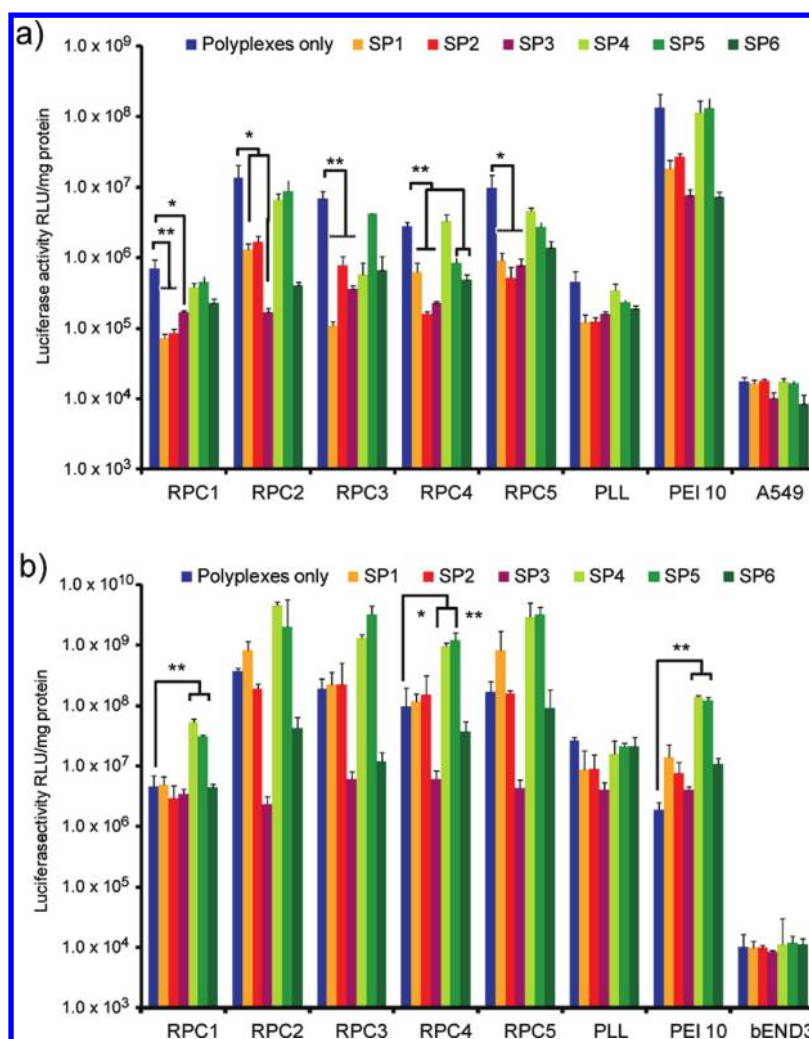


**Figure 4.** Expression of luciferase, as monitored by light production, following incubation of polymer/pDNA complexes in A549 (a) or bEND.3 (b) cells. Dark-blue bars show expression induced by RPC/DNA complexes alone, while SP1–SP3 shield polymers are nondegradable and SP4–SP6 polymers are acid-labile. Results are mean  $\pm$  SE values from triplicate determinations. Statistically significant differences in light production comparing polymer/DNA complexes coated with the varying shield polymers are indicated by a single star (\*,  $p < 0.05$ ) or a double star (\*\*,  $p < 0.01$ ) based on analysis of variants (ANOVA) with a Dunnett post-test.

difficulty in unpackaging the outer layer cross-linked by this tetrafunctional oxirane polymer compared to the bis oxirane analogues SP4 and 5 ( $^1\text{H}$  NMR spectra of hydrolysis products, data not shown). Nevertheless, the fact that SP4 and SP5-coated polymer/DNA complexes were in general as active as their noncoated counterparts and more effective than complexes coated with nondegradable shield polymers was a promising indicator for the acetal-coating polymer strategy.

For bEND.3 cells, there was no statistically significant decrease in light production due to coating of the polymer/DNA complexes with any of the coating polymers, although there were significant increases in transfection efficiency for RPC1 and RPC4/DNA complexes coated with SP4 and 5. Complexes of RPCs 2–5 coated with polymer SP3 appeared less efficient at inducing luciferase production than those with SP1 and SP2, but differences between these values were not significant to a confidence level of 0.05. A mechanism for the subtle differences in transfection efficiencies for RPCs 2–5 (i.e., the lysine-histidine copolymers) in bEND.3 cells when coated with hydrophilic shield polymers is the subject of ongoing studies in our laboratories; however, the differences in light production in this cell line likely indicate a higher degree of reductive unpackaging than in other

cell lines, as found in the relative pattern of gene expression for the underlying polypeptide cores, i.e., RPCs 1–5 observed for our prior studies in the same cell lines.<sup>41</sup> This suggested that the cleavable coat polymers likely did not change the final DNA release mechanisms and subsequent transcription processes, with the most “blocky” polypeptide, RPC2 (poly( $\text{CK}_4\text{H}_4\text{C}$ )) being the most active core vector.

All the RPC/DNA complexes were well-tolerated by both cell lines as indicated by MTS metabolic activity assays (Supporting Information). Although significant toxicities were observed when testing cross-linked PLL and PEI/DNA polyplexes, the histidine-rich RPCs were found to have low overall toxicities when formulated as polyplexes and when coated with cross-linking polymers.

Complexation of the polycations and coating of the complexes reduced hemolysis of human erythrocytes to less than 6% of sample for all the complexes, compared to a hemolysis value of >14% for free poly L-lysine, demonstrating the better cytocompatibility of the complexes and their PEG-shielded analogues as opposed to the native RPCs alone.

**3.4. Retargeting of Cleavable Polymer Coated RPC/DNA Complexes.** Having demonstrated the core and shield

chemistries for the virus mimetics, we introduced cell targeting functionality at the surface of the complexes, using transferrin (Tf) to interact with the Tf-receptor known to be overexpressed on many cancerous cells. This was accomplished by simply adding Tf to the RPC/DNA complexes at the same time as the coating polymer, allowing amine residues of both protein and RPC polypeptide to react with the oxirane groups at the shield polymer termini. The Tf-tagged coated RPC/DNA complexes were separated from unbound Tf and shield polymers, as well as any residual excess reducible polycation using gel filtration and quantification of bound and unbound Tf was achieved via parallel experiments with FITC-labeled Tf (Supporting Information).

Specificity of uptake with Tf-tagged polymer/DNA complexes was established through assays with the human colon carcinoma cell-line (HCT116), which expresses high levels of transferrin receptors.<sup>44</sup> Optimization studies were initially carried out with PEI as an easily accessible core component and SP5 as the reactive coating polymer as this previously gave the best transfection and cell-viability results. Uptake of the Tf-tagged complexes into HCT116 cells occurred in a dose-dependent manner and was suppressed by addition of free Tf to the same cell line also in a dose-dependent way (Supporting Information). These experiments validated the retargeting of the viral mimetic carriers through surface-tagging with a ligand.

The culminating experiments set out to test the efficacy of uptake of the RPC/DNA complexes, when coated and tagged, into Tf-receptor positive cell lines, HCT116 (colorectal carcinoma) and HL-60 (human promyelocytic leukemia). Transfection conditions were derived from those used in prior assays to allow comparison of efficacy across the range of RPCs 1–5 and the coating polymers for these transferrin-receptor-positive cell lines. However, slightly higher cell seeding densities ( $10^5$  to  $5 \times 10^5$  cells per well compared to  $7 \times 10^4$  cells per well for A549 and b,END 3 cells) and 24-well plates were used for HCT116 and HL-60 cells owing to differences in their adherence to plate-reader wells. These assays were thus quantitatively comparative for the RPCs and coating polymers for HCT116 and HL-60 cells only.

Polyplexes of RPCs1–5, PLL, and PEI/DNA coated with bis(oxiraneacetal)–PEG polymer SP5 were slightly less effective in transfecting Tf-positive HCT116 and HL-60 cell lines (Figure 5a) compared to noncoated polyplexes derived from the same polycations. Decreases in luciferase expression of  $\sim 5$ –190-fold were observed in HCT116 cells compared to noncoated analogues, but conjugation of Tf to the same RPC/DNA polyplexes (at optimized Tf/polyplex ratios) either partially restored or increased transgene expression compared to noncross-linked analogues. This occurred in the case of Tf-targeted polyplexes of RPC4 and PEI/DNA, which showed enhancements in luciferase activity of  $\sim 50$ - and 273-fold compared to their SP5 cross-linked analogues respectively. A similar pattern was observed for HL-60 cells (Figure 5b), in which SP5 cross-linked systems moderately decreased transfection efficiency, while tagging with Tf restored or slightly increased the luciferase activity compared to SP5 cross-linked polyplexes ( $\sim 3$ –12 fold). Overall transfection efficacy correlated to the growth rate of the tested cell lines, which was in the order HCT116 > HL-60 as expected based on the function of the Tf-receptor.

Fluorescence microscopy was used to evaluate polyplex uptake over 1–24 h (Figure 5c, i–iii). For SP5 coated RPC2/DNA polyplexes (containing DNA labeled with YOYO-1), polyplex uptake was minimal up to 4 h (Figure 5c column ii).

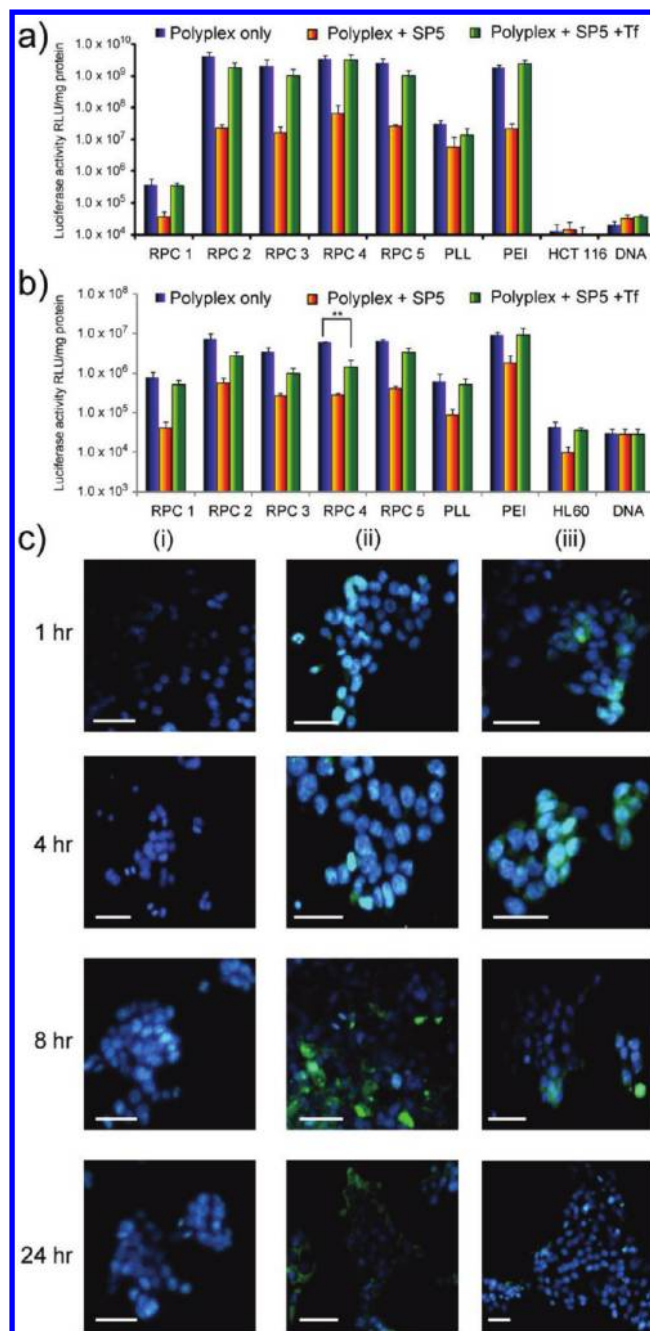


**Figure 5.** (a,b) Luciferase activity of polyplexes of RPCs1–5, PLL ( $N/P = 5$ ), and PEI ( $N/P = 10$ )/DNA, non-(NC), SP5 cross-linked, and Tf-targeted are shown 48 h after transfecting HCT116 (a) and HL-60 (b) cells. Results are mean  $\pm$  SE values from triplicate determinations. Statistically significant differences in light production comparing polymer/DNA complexes coated with the varying shield polymers are indicated by a single star (\*,  $p < 0.05$ ) or a double star (\*\*,  $p < 0.01$ ) based on analysis of variants (ANOVA) with a Dunnett post-test. (c) Fluorescence micrographs of (i) HCT116 cells only (control), and following transfection with (ii) SP5 cross-linked RPC2/DNA polyplexes (DNA labeled with YOYO-1) and (iii) Tf-targeted SP5 cross-linked RPC2/DNA polyplexes (Tf labeled with FITC). Following transfection, HCT116 cells were washed and fixed with 1% (w/v) PFA at specified time intervals. Scale bar: 50  $\mu$ m.

Uptake of these polyplexes increased as indicated by higher cytosolic YOYO-1 fluorescence in images taken after 8 and 24 h. By contrast, Tf-targeted SP5 coated RPC2/DNA polyplexes (containing Tf labeled with FITC) were internalized rapidly, as

evidenced by FITC fluorescence in the cytosol of HCT116 cells after 1 h (Figure 5c column iii). Cytosolic fluorescence diminished after 8 h and was almost undetectable after 1 day. MTS assays (Supporting Information) showed that all the noncoated, coated, and retargeted viral mimetic carriers were well tolerated by HCT116 and HL-60 cells, indicating transfection efficacy was not compromised by toxicity.

#### 4. DISCUSSION

We commenced building the core using lysine and histidine-based polycations, linked by intracellularly reducible disulfides from terminal cysteine residues. These RPC materials<sup>23,45</sup> had previously been shown by gel electrophoresis, DLS, and AFM to degrade to oligopeptide components under biologically relevant reducing conditions<sup>41</sup> (5 mM GSH) and also to display membrane-penetrating activity combined with good cytocompatibility and efficient transfection<sup>41,46</sup> and so were good candidates for the vector cores.

We then sought to coat the polyelectrolyte complexes formed between DNA and the various RPCs in order to stabilize them against both physicochemical and biological challenge. We required a shell or “shield” polymer to cross-link partially the polyelectrolyte complexes after they had been formed and to mask or sterically shield their overall positive charge. This shielding polymer also needed to be easy to prepare, to be biocompatible and capable of further derivatization with targeting groups once in place. This is because polymers used previously to coat nanoparticle vectors have been shown not only to decrease undesirable interactions with blood cells and plasma components but also to reduce their interaction with negatively charged membranes in the targeted tissues, leading to lower overall transfection.<sup>25,28</sup> The retargeting of the coated polyplexes thus needed to be considered, for example by conjugating ligands for specific cell-surface receptors to the shield polymer, during or after the shell cross-linking process. Such a method has been found to restore transgene expression in target cells.<sup>26,40</sup> We accordingly needed a reactive shielding polymer capable of simultaneous or posthoc conjugation to both targeting ligands and excess amine groups on the RPC/DNA complexes. Crucially, however, this polymer also needed to exhibit the viral-mimetic behavior of self-release once inside a cell. Prior studies have indicated that polyplexes coated with noncleavable polymers possess a lower ability to escape endosomal barriers, again leading to a loss in transfection efficiency.<sup>29</sup> We therefore required a material to coat, shield, and retarget the RPC/DNA complexes and then self-release, to allow the membrane-disrupting peptidic core to transport the nucleic acid cargo, prior to the core itself decomposing by reductive cleavage in the cytosol, to liberate DNA.

Poly(2-hydroxypropylmethacrylamide) (pHPMA) coating polymers attached to polyplexes by biodegradable tetrapeptides (Gly-Phe-Leu-Gly) have been specifically uncoated by the lysosomal enzyme cathepsin B and exhibited higher transgene expression compared to noncleavable controls.<sup>26</sup> Acid-hydrolyzable PEG shields have also been used to coat gene delivery vectors, utilizing the endosomal pH drop as a stimulus for uncoating.<sup>6,29–38</sup> These studies have shown the efficacy of the general strategy of reversibly coating a gene carrier to enhance transgene expression.<sup>39</sup> In our case, we needed chemistries that would allow facile coating of preformed complexes but also a “one-pot” route that would enable conjugation of targeting ligands in the same step as the coating reaction. In addition, we needed to demonstrate that each component in our modular

gene delivery system functioned as intended, i.e., that the viral mimetic chemistries each played a part in the final function of the coated and retargeted polyplexes.

The concepts underlying this strategy are shown in Figure 1 and the chemistries in Figure 2. The facile reaction of oxiranes with amines under ambient conditions<sup>47</sup> suggested that the coating “shield” materials could be based around polymers with an oxirane group at each end, while the previous work by Gillies et al.<sup>38,48</sup> had demonstrated the utility of the acetal degradable link. Several oxirane-tipped oligo- and poly(ethyleneglycol)s were available commercially, thus we used three representative compounds as control shield polymers (SP1–3, Figure 2) and prepared the analogous acetal-linked (oxirane)-tipped oligo- and poly(ethyleneglycol)s (SP4–6) by adapting a reported route.<sup>43</sup> Polymers SP4–6 were found by <sup>1</sup>H NMR to be stable to hydrolysis at pH 7.4 for several days (Supporting Information), and polyplexes of all RPCs with DNA after reaction with with these shield polymers were similar in structure and morphology to the same polyplexes reacted with the noncleavable polymers SP1–3 as shown by AFM in aqueous conditions (Figure 2c). In addition, particle sizes for RPCs 1–5 reacted with SP4–6 were shown in some cases by AFM (Supporting Information) to be slightly larger than those for the noncoated RPCs, suggesting the presence of an outer shield layer to these complexes. These differences (up to 60 nm in measured diameter) were not, however, closely correlated with molar mass of the shield polymers. This implied that the coating reactions were not simply taking place at the outer layer of the polyplexes to generate a “corona” whose size is dependent on the chain length of the shield polymers. In all cases, the polyplexes studied in AFM were separated away from excess polycation, used in the polyplex formation, and any residual shield polymer, by passage of the polyplexes through a gel filtration column. This ensured that any changes in particle size observed in AFM were likely a result of interparticle coating and shell cross-linking rather than intercomplex bridging.

The stabilities of the shield polymers to plasma pH (no hydrolysis at pH 7.4 for >48 h) were in marked contrast to those at a simulated endosomal pH of 5.6. Proton signals in <sup>1</sup>H NMR spectra due to the presence of hemiacetal and acetaldehyde arising from shield polymer hydrolysis at pH 5.6 were apparent within 1 h (Supporting Information). Although complete hydrolysis of SP4 and SP5 at pH 5.6 took >24 h (Supporting Information), agarose gel electrophoresis studies and AFM in aqueous solution showed unpackaging of DNA in much shorter time scales for these degradable polymers. In Figure 3a–d, the differences in stability of polypeptide/DNA RPCs 1–5 with representative noncleavable (SP1 and SP2) compared to cleavable (SP4, SP5) coating polymers can be seen. RPCs 1–5 coated with SP1 and SP2 (Figure 3a,c) retained DNA in their complexes under challenge by a competing polyanion, polyaspartic acid (PAA), at pH 7.4 and 5.6 (lanes 2 and 3 for each RPC), but released DNA on exposure to a strong reducing agent dithiothreitol (DTT, lanes 4 for each RPC). In parts b and d of Figure 3, the same assays, carried out on RPCs1–5 coated with acid-labile SP4 and SP5, showed that DNA was released, as apparent in lane 3 for each RPC, indicating loss of coating polymer and destabilization of the complex by competing PAA at pH 5.6 only. The fact that in all cases the complexes could be unpackaged completely by the reducing agent (Figure 3a–d, lanes 4) suggested that the cross-linking with the shield polymers was not sufficient to “lock” the DNA in irreversibly. However, the release of DNA from the

cleavable shield polymer-coated RPCs at pH 5.6 but not from the noncleavable polymer-coated complexes under the same conditions demonstrated that the shield polymer coating was sufficient protection in the absence of an acidic challenge. AFM data (Figure 3e) showed the emergence of DNA strands from the RPC1 polyplexes coated with shield polymer SP5 after 120 min at pH 5.6. These results together indicated that the RPC polyplexes coated with the oxirane-tipped oligo- and poly-(ethyleneglycols) were stable against competing polyanion challenge at pH 7.4 and that the cleavable shield polymers were sufficiently labile *in vitro* to enable release of DNA under simulated endosomal pH.

The transfection data (Figure 4) showed that, in general, the core components (i.e., RPCs 1–5) displayed transfection activities essentially independent of the presence of bis(oxiraneacetal)–PEG cleavable coat polymers (SP4 and 5) but were diminished in activity when coated with nondegradable oxiranePEGs (SP1–3), although there were some individual variations for RPCs 3 and 4. This we suggest was due to shedding of at least some of the acid-labile PEG-coats intracellularly, as supported by the prior <sup>1</sup>H NMR, gel retardation, and AFM assays, which clearly showed DNA release from the bis(oxiraneacetal)–PEG coated polyplexes, but not from the noncleavable coated polyplexes, over the same time scales as the transfection assays. Uptake of complexes and transgene expression was nevertheless observed, albeit to a lesser extent, with the noncleavable coated polyplexes, which we attribute to the permeability of the nanoparticles as a result of an incomplete surface coat and access to the polypeptide domains. This was in accord with the gel retardation assays in which reducing agents were able to unpack DNA even with the noncleavable shield polymer-coated RPCs. However, the fact that overall transfection was higher for the cleavable shield polymer (SP4,5)-coated RPCs was encouraging, as it indicated a clear advantage for coating the RPCs with the degradable material. These transfection experiments were carried out in reduced serum media in order to establish baseline transfection efficiencies, but the increased stability of the SP4–6 coated polyplexes against polyanion challenge as shown in Figure 3, combined with the better overall transgene expression with these systems, provided further support for the multicomponent vector strategy. The final data required prior to vector retargeting experiments were results demonstrating that the polyplexes did not reduce cell viability. No significant decrease in viability of either the A549 or bEND.3 cells was observed when incubated with any of the RPCs prereacted with shield polymers, except for those RPCs coated with SP6. Overall, metabolic activities following treatment with the coated RPCs were in close agreement with our previous data for the RPCs 1–5 alone in these cell lines.

Having established the efficacy and biocompatibility of the core–shield systems, we conducted experiments with polyplexes tagged with the iron-binding and transport protein transferrin, in two cell lines, HCT116 and HL-60, known to express the transferrin (Tf) receptor. The “one-pot” strategy of adding transferrin and oxirane-tipped shield polymer to the polyplexes was found to be effective, as the presence of FITC-Tf on the complexes was clearly demonstrated in spectroscopic assays and microscopy images. In addition, Tf-tagged and shield-polymer-coated RPCs could be separated and purified on gel filtration columns as before, thus removing any potential competing factors in cell uptake and transfection assays. The specificity of Tf-mediated uptake and transfection in the HCT116 cell line was evaluated using Tf-tagged SP5-coated PEI (Supporting Information) wherein polyplexes with increased amounts of conjugated Tf showed progressively

increased transfection (dose dependent) until a plateau level. Addition of free Tf in the presence of the same Tf-tagged polyplexes resulted in a dose-dependent reduction in transfection. The use of transgene expression as a reporter in these assays, i.e., many steps downstream of cell entry, was strongly suggestive that selective uptake via the Tf-mediated endocytic pathway was a key limiting factor in the activity of these complexes. Consideration of  $\zeta$  potentials (+5–10 mV across the full range of polyplexes) in these assays did indicate that the positive charges from the peptidic cores extended, at least partially, to the surfaces and were not fully shielded by the PEG coating layers. As a consequence, it is likely that uptake by passive endocytosis also occurred for these systems, although in general,  $\zeta$  potentials of coated polyplexes were less positive than those for noncoated complexes. More detailed experiments with the full range of RPCs with the shield polymer SP5 and with or without Tf in HCT116 and HL-60 cells highlighted again the role of retargeting by addition of Tf. As apparent in Figure 5 a,b, transgene expression of all the RPCs alone followed a similar overall qualitative pattern to those observed in A549 and bEND.3 cells, with the more “blocky” poly(CK<sub>4</sub>H<sub>4</sub>C) (RPC2) peptide cores being most effective and the (CK<sub>8</sub>C)<sub>n</sub> (RPC1) generating lowest luciferase expression. Coating with SP5 alone reduced transgene expression, as expected on the grounds of reduced overall uptake, but addition of Tf restored transfection activity in all cases. Importantly, addition of the shield polymers and Tf did not affect cell viability (Supporting Information), and for all the RPCs, viability was better for these complexes than for those with PEI and PLL while maintaining the same, or higher, overall transfection activity.

Further support for the success of the retargeting module was obtained from microscopy experiments (Figure 5c) with slower uptake of SP5 coated RPC2/DNA polyplexes compared to the Tf-tagged counterparts. The effect of particle size was not likely to have been important, as these were not significantly different for coated vs noncoated polyplexes across the set and the overall size ranges (100–140 nm diameter, Supporting Information) would not be expected to change the uptake pathways.<sup>49</sup> The Tf-tagged SP5-coated RPC2/DNA complexes were larger than the corresponding SP5-RPC2/DNA complexes, and this may have moderated the ratio of caveolae-mediated compared to clathrin-mediated uptake; however, it was notable that for both Tf-receptor expressing cell lines, transfection efficiency was enhanced by ligand functionalization compared to the nonfunctionalized coated particles. In addition, the decrease in cytosolic fluorescence from HCT116 cells 1 day after exposure to Tf-targeted polyplexes suggested a role for specific uptake and recycling via the Tf-receptor. Cleavage of SP5 cross-links could have taken place during the 48 h total time-course of the microscopy experiments (because the Tf-recycling pathway involves acidification inside endosomal vesicles). This in turn would have led to removal of Tf from the surface of polyplexes to allow FITC-Tf to be recycled by the Tf-receptor pathway and subsequent removal of the fluorescent protein during the washing stages prior to imaging. The pH-dependent fluorescence of FITC complicated attempts to follow the intracellular passage of the complexes by confocal microscopy, but the combination of enhanced transfection in the Tf-tagged cells with the results of competition experiments involving free Tf were strongly supportive of successful retargeting of the multicomponent complexes.

When considered as a whole, the efficacy of the multicomponent strategy was demonstrated *in vitro*, but some caveats remain for *in vivo* studies. The coated polyplexes in

these studies were stable against challenge by polyanions but for in vivo use would need to retain their colloidal stability in the presence of serum proteins, and thus more extended coronae of hydrophilic coating polymers might be required. In addition, the hydrolysis rates of the acetal groups in the shield polymers were sufficiently fast to show some unpacking of DNA in vitro, but might need to be optimized for in vivo use, as intracellular trafficking takes place over time scales of minutes rather than hours. These studies are ongoing in our laboratories and will be reported in a future manuscript. Nevertheless, the combination of functionalities, built in a stepwise fashion, is promising as a platform for delivery of a range of other biotherapeutics, as the chemistries of assembly are all compatible with biopolymers such as siRNA as well as DNA.

## 5. CONCLUSIONS

In conclusion, we have shown that it is possible to generate synthetic polymers with viral mimetic chemistries via facile stepwise assembly of modular core, shell, and targeting components. Overall transfection levels in a range of cancer-relevant cell-lines were as high, or higher, than those achieved using the current best exemplar synthetic vectors PLL or PEI but with significantly enhanced tolerability as measured by retention of metabolic activity. The ability to prepare the vectors from easily variable families of peptidic cores, and with acetalized PEGs accessible from many different polyol precursors, combined with in situ functionalization of the oxirane-coating polymers enabling any amine- or thiol-tipped targeting ligand to be placed on the polyplex surfaces under ambient conditions, offers many advantages over existing synthetic gene carriers. Experiments to evaluate the in vivo efficacy of these multicomponent viral mimetics are developing, but the hemocompatibility, low toxicity, and transfection efficacy in cell culture, and at doses (0.5–4  $\mu\text{g}$  of DNA) used in gene therapy trials previously, hold promise that these systems may be active in vivo as well as in vitro

## ■ ASSOCIATED CONTENT

### ■ Supporting Information

$^1\text{H}$  NMR, GPC chromatograms, and  $^{13}\text{C}$  NMR of the polymers, MTS assays, DLS, and AFM data for complexes, gel retardation and hemocompatibility assays. This material is available free of charge via the Internet at <http://pubs.acs.org>.

## ■ AUTHOR INFORMATION

### Corresponding Author

\*E-mail: [cameron.alexander@nottingham.ac.uk](mailto:cameron.alexander@nottingham.ac.uk)

## ■ ACKNOWLEDGMENTS

This work was supported by the Biotechnology and Biological Sciences Research Council (grant BBC5158551), the Engineering and Physical Sciences Research Council (grant EP/H005625/1), and by a scholarship to M.S. from the Egyptian Government. We also thank Christine Grainger-Boulthby for technical help, Drs. Sivanand Pennadam and Ji-Won Pack for preliminary experiments on coating polymer synthesis, and Neil Spencer and Peter Ashton for NMR and mass spectrometry.

## ■ REFERENCES

- (1) Petros, R. A.; DeSimone, J. M. Strategies in the design of nanoparticles for therapeutic applications. *Nature Rev. Drug Discovery* **2010**, *9*, 615–627.
- (2) Gao, W.; Chan, J. M.; Farokhzad, O. C. pH-Responsive Nanoparticles for Drug Delivery. *Mol. Pharmaceutics* **2010**, *7* (6), 1913–1920.
- (3) Meng, F.; Zhong, Z.; Feijen, J. Stimuli-Responsive Polymersomes for Programmed Drug Delivery. *Biomacromolecules* **2009**, *10* (2), 197–209.
- (4) Gao, K.; Huang, L. Nonviral Methods for siRNA Delivery. *Mol. Pharmaceutics* **2009**, *6* (3), 651–658.
- (5) Douglas, K. L. Toward development of artificial viruses for gene therapy: a comparative evaluation of viral and non-viral transfection. *Biotechnol. Prog.* **2008**, *24* (4), 871–883.
- (6) Smith, A. E.; Helenius, A. How Viruses Enter Animal Cells. *Science* **2004**, *304* (5668), 237–242.
- (7) Manno, C. S.; Arruda, V. R.; Pierce, G. F.; Glader, B.; Ragni, M.; Rasko, J.; Ozelo, M. C.; Hoots, K.; Blatt, P.; Konkle, B.; Dake, M.; Kaye, R.; Razavi, M.; Zajko, A.; Zehnder, J.; Nakai, H.; Chew, A.; Leonard, D.; Wright, J. F.; Lessard, R. R.; Sommer, J. M.; Tigges, M.; Sabatino, D.; Luk, A.; Jiang, H.; Mingozzi, F.; Couto, L.; Ertl, H. C.; High, K. A.; Kay, M. A. Successful transduction of liver in hemophilia by AAV-Factor IX and limitations imposed by the host immune response. *Nature Med.* **2006**, *12* (3), 342–347.
- (8) Cavazzana-Calvo, M.; Fischer, A. Gene therapy for severe combined immunodeficiency: are we there yet? *J. Clin. Invest.* **2007**, *117* (6), 1456–1465.
- (9) Matsumoto, S.; Christie, R. J.; Nishiyama, N.; Miyata, K.; Ishii, A.; Oba, M.; Koyama, H.; Yamasaki, Y.; Kataoka, K. Environment-Responsive Block Copolymer Micelles with a Disulfide Cross-Linked Core for Enhanced siRNA Delivery. *Biomacromolecules* **2009**, *10* (1), 119–127.
- (10) Takae, S.; Miyata, K.; Oba, M.; Ishii, T.; Nishiyama, N.; Itaka, K.; Yamasaki, Y.; Koyama, H.; Kataoka, K. PEG-detachable polyplex micelles based on disulfide-linked block cationomers as bioresponsive nonviral gene vectors. *J. Am. Chem. Soc.* **2008**, *130* (18), 6001–6009.
- (11) De Smedt, S. C.; Demeester, J.; Hennink, W. E. Cationic Polymer Based Gene Delivery Systems. *Pharm. Res.* **2000**, *17* (2), 113–126.
- (12) Thomas, M.; Ge, Q.; Lu, J. J.; Chen, J. Z.; Klibanov, A. M. Cross-Linked Small Polyethylenimines: While Still Nontoxic, Deliver DNA Efficiently to Mammalian Cells in Vitro and in Vivo. *Pharm. Res.* **2005**, *22* (3), 373–380.
- (13) Lee, Y.; Mo, H.; Koo, H.; Park, J. Y.; Cho, M. Y.; Jin, G. w.; Park, J. S. Visualization of the Degradation of a Disulfide Polymer, Linear Poly(ethylenimine sulfide), for Gene Delivery. *Bioconjugate Chem* **2007**, *18* (1), 13–18.
- (14) Drake, C. R.; Aissaoui, A.; Argyros, O.; Serginson, J. M.; Monnery, B. D.; Thanou, M.; Steinke, J. H. G.; Miller, A. D. Bioresponsive Small Molecule Polyamines as Noncytotoxic Alternative to Polyethylenimine. *Mol. Pharmaceutics* **2010**, *7* (6), 2040–2055.
- (15) Mok, H.; Veisoh, O.; Fang, C.; Kievit, F. M.; Wang, F. Y.; Park, J. O.; Zhang, M. pH-Sensitive siRNA Nanovector for Targeted Gene Silencing and Cytotoxic Effect in Cancer Cells. *Mol. Pharmaceutics* **2010**, *7* (6), 1930–1939.
- (16) Davis, M. E.; Zuckerman, J. E.; Choi, C. H. J.; Seligson, D.; Tolcher, A.; Alabi, C. A.; Yen, Y.; Heidel, J. D.; Ribas, A. Evidence of RNAi in humans from systemically administered siRNA via targeted nanoparticles. *Nature* **2010**, *464* (7291), 1067–1070.
- (17) Semple, S. C.; Akinc, A.; Chen, J. X.; Sandhu, A. P.; Mui, B. L.; Cho, C. K.; Sah, D. W. Y.; Stebbing, D.; Crosley, E. J.; Yaworski, E.; Hafez, I. M.; Dorkin, J. R.; Qin, J.; Lam, K.; Rajeev, K. G.; Wong, K. F.; Jeffs, L. B.; Nechev, L.; Eisenhardt, M. L.; Jayaraman, M.; Kazem, M.; Maier, M. A.; Srinivasulu, M.; Weinstein, M. J.; Chen, Q. M.; Alvarez, R.; Barros, S. A.; De, S.; Klimuk, S. K.; Borland, T.; Kosovrsti, V.; Cantley, W. L.; Tam, Y. K.; Manoharan, M.; Ciufolini, M. A.; Tracy, M. A.; de Fougerolles, A.; MacLachlan, I.; Cullis, P. R.; Madden, T. D.;

Hope, M. J. Rational design of cationic lipids for siRNA delivery. *Nature Biotechnol.* **2010**, *28* (2), 172–U18.

(18) Chang, K.-L.; Higuchi, Y.; Kawakami, S.; Yamashita, F.; Hashida, M. Efficient Gene Transfection by Histidine-Modified Chitosan through Enhancement of Endosomal Escape. *Bioconjugate Chem.* **2010**, *21* (6), 1087–1095.

(19) Petersen, H.; Merdan, T.; Kunath, K.; Fischer, D.; Kissel, T. Poly(ethylenimine-co-L-lactamide-co-succinamide): a biodegradable polyethylenimine derivative with an advantageous pH-dependent hydrolytic degradation for gene delivery. *Bioconjugate Chem.* **2002**, *13* (4), 812–821.

(20) Boeckle, S.; von Gersdorff, K.; van der Piepen, S.; Culmsee, C.; Wagner, E.; Ogris, M. Purification of polyethylenimine polyplexes highlights the role of free polycations in gene transfer. *J. Gene Med.* **2004**, *6* (10), 1102–1111.

(21) Chollet, P.; Favrot, M. C.; Hurbin, A.; Coll, J. L. Side-effects of a systemic injection of linear polyethylenimine–DNA complexes. *J. Gene Med.* **2002**, *4* (1), 84–91.

(22) Plank, C.; Mechtler, K.; Szoka, F. C.; Wagner, E. Activation of the complement system by synthetic DNA complexes: a potential barrier for intravenous gene delivery. *Hum. Gene Ther.* **1996**, *7* (12), 1437–1446.

(23) McKenzie, D. L.; Kwok, K. Y.; Rice, K. G. A potent new class of reductively activated peptide gene delivery agents. *J. Biol. Chem.* **2000**, *275* (14), 9970–9977.

(24) Neu, M.; Germershaus, O.; Mao, S.; Voigt, K.-H.; Behe, M.; Kissel, T. Crosslinked nanocarriers based upon poly(ethylene imine) for systemic plasmid delivery: in vitro characterization and in vivo studies in mice. *J. Controlled Release* **2007**, *118* (3), 370–380.

(25) Oupicky, D.; Carlisle, R. C.; Seymour, L. W. Triggered intracellular activation of disulfide crosslinked polyelectrolyte gene delivery complexes with extended systemic circulation in vivo. *Gene Ther.* **2001**, *8* (9), 713–724.

(26) Dash, P. R.; Read, M. L.; Fisher, K. D.; Howard, K. A.; Wolfert, M.; Oupicky, D.; Subr, V.; Strohal, J.; Ulbrich, K.; Seymour, L. W. Decreased binding to proteins and cells of polymeric gene delivery vectors surface modified with a multivalent hydrophilic polymer and retargeting through attachment of transferrin. *J. Biol. Chem.* **2000**, *275* (6), 3793–3802.

(27) Ogris, M.; Brunner, S.; Schüller, S.; Kircheis, R.; Wagner, E. PEGylated DNA/transferrin-PEI complexes: reduced interaction with blood components, extended circulation in blood and potential for systemic gene delivery. *Gene Ther.* **1999**, *6* (4), 595–605.

(28) Erbacher, P.; Bettinger, T.; Belguise-Valladier, P.; Zou, S.; Coll, J. L.; Behr, J. P.; Remy, J. S. Transfection and physical properties of various saccharide, poly(ethylene glycol), and antibody-derivatized polyethylenimines (PEI). *J. Gene Med.* **1999**, *1* (3), 210–222.

(29) Knorr, V.; Allmendinger, L.; Walker, G. F.; Paintner, F. F.; Wagner, E. An acetal-based PEGylation reagent for pH-sensitive shielding of DNA polyplexes. *Bioconjugate Chem.* **2007**, *18* (4), 1218–1225.

(30) Kale, A. A.; Torchilin, V. P. Design, synthesis, and characterization of pH-sensitive PEG-PE conjugates for stimuli-sensitive pharmaceutical nanocarriers: the effect of substitutes at the hydrazone linkage on the pH stability of PEG-PE conjugates. *Bioconjugate Chem.* **2007**, *18* (2), 363–370.

(31) Walker, G. F.; Fella, C.; Pelisek, J.; Fahrmeir, J.; Boeckle, S.; Ogris, M.; Wagner, E. Toward synthetic viruses: endosomal pH-triggered deshielding of targeted polyplexes greatly enhances gene transfer in vitro and in vivo. *Mol. Ther.* **2005**, *11* (3), 418–425.

(32) Shin, J.; Shum, P.; Thompson, D. H. Acid-triggered release via dePEGylation of DOPE liposomes containing acid-labile vinyl ether PEG-lipids. *J. Controlled Release* **2003**, *91* (1–2), 187–200.

(33) Choi, J. S.; MacKay, J. A.; Szoka, F. C. Low-pH-sensitive PEG-stabilized plasmid–lipid nanoparticles: preparation and characterization. *Bioconjugate Chem.* **2003**, *14* (2), 420–429.

(34) Li, W.; Huang, Z.; MacKay, J. A.; Grube, S.; Szoka, F., C. Jr. Low-pH-sensitive poly(ethylene glycol) (PEG)-stabilized plasmid

nanolipoparticles: effects of PEG chain length, lipid composition and assembly conditions on gene delivery. *J. Gene Med.* **2005**, *7* (1), 67–79.

(35) Hoffman, A.; Stayton, P.; Press, O.; Murthy, N.; Lackey, C.; Cheung, C.; Black, F.; Campbell, J.; Fausto, N.; Kyriakides, T.; Bornstein, P. Bioinspired polymers that control intracellular drug delivery. *Biotechnol. Bioprocess Eng.* **2001**, *6* (4), 205–212.

(36) Murthy, N.; Campbell, J.; Fausto, N.; Hoffman, A. S.; Stayton, P. S. Design and synthesis of pH-responsive polymeric carriers that target uptake and enhance the intracellular delivery of oligonucleotides. *J. Controlled Release* **2003**, *89* (3), 365–374.

(37) Murthy, N.; Campbell, J.; Fausto, N.; Hoffman, A. S.; Stayton, P. S. Bioinspired pH-responsive polymers for the intracellular delivery of biomolecular drugs. *Bioconjugate Chem.* **2003**, *14* (2), 412–419.

(38) Gillies, E. R.; Goodwin, A. P.; Frechet, J. M. J. Acetals as pH-sensitive linkages for drug delivery. *Bioconjugate Chem.* **2004**, *15* (6), 1254–1263.

(39) Behr, J.-P. The proton sponge: a trick to enter cells the viruses did not exploit. *CHIMIA, Int. J. Chem.* **1997**, *51* (1–2), 34–36.

(40) Stevenson, M.; Ramos-Perez, V.; Singh, S.; Soliman, M.; Preece, J. A.; Briggs, S. S.; Read, M. L.; Seymour, L. W. Delivery of siRNA mediated by histidine-containing reducible polycations. *J. Controlled Release* **2008**, *130* (1), 46–56.

(41) Nasanit, R.; Iqbal, P.; Soliman, M.; Spencer, N.; Allen, S.; Davies, M. C.; Briggs, S. S.; Seymour, L. W.; Preece, J. A.; Alexander, C. Combination dual responsive polypeptide vectors for enhanced gene delivery. *Mol. BioSystems* **2008**, *4*, 741–745.

(42) Ogris, M.; Steinlein, P.; Kurs, M.; Mechtler, K.; Kircheis, R.; Wagner, E. The Size of DNA/Transferrin-PEI Complexes using PEI-transferrin-DNA complexes is an Important Factor for Gene Expression in Cultured Cells. *Gene Ther.* **1998**, *5*, 1425–1433.

(43) Fitton, A.; Hill, J.; Jane, D.; Millar, R. Synthesis of simple oxetanes carrying reactive 2-substituents. *Synthesis* **1987**, *12*, 1140–1142.

(44) Calzolari, A.; Deaglio, S.; Maldì, E.; Cassoni, P.; Malavasi, F.; Testa, U. TfR2 expression in human colon carcinomas. *Blood Cells, Mol. Dis.* **2009**, *43* (3), 243–249.

(45) Mckenzie, D. L.; Smiley, E.; Kwok, K. Y.; Rice, K. G. Low Molecular Weight Disulfide Cross-Linking Peptides as Nonviral Gene Delivery Carriers. *Bioconjugate Chem.* **2000**, *11* (6), 901–909.

(46) Soliman, M.; Nasanit, R.; Allen, S.; Davies, M. C.; Briggs, S. S.; Seymour, L. W.; Preece, J. A.; Alexander, C. Interaction of Reducible Polypeptide Gene Delivery Vectors with Supported Lipid Bilayers: Pore Formation and Structure–Function Relationships. *Soft Matter* **2010**, *6* (11), 2517–2524.

(47) Azizi, N.; Saidi, M. R. Highly chemoselective addition of amines to epoxides in water. *Org. Lett.* **2005**, *7* (17), 3649–3651.

(48) Gillies, E. R.; Frechet, J. M. J. pH-Responsive copolymer assemblies for controlled release of doxorubicin. *Bioconjugate Chem.* **2005**, *16* (2), 361–368.

(49) Pouton, C. W.; Seymour, L. W. Key issues in non-viral gene delivery. *Adv. Drug Delivery Rev.* **2001**, *46* (1–3), 187–203.